



Oxygen nonstoichiometry, thermal expansion and high-temperature electrical properties of layered $\text{NdBaCo}_2\text{O}_{5+\delta}$ and $\text{SmBaCo}_2\text{O}_{5+\delta}$

T.V. Aksenova^a, L.Yu. Gavrilova^a, A.A. Yaremchenko^b, V.A. Cherepanov^{a,*}, V.V. Kharton^b

^a Department of Chemistry, Ural State University, Lenin av. 51, Ekaterinburg, Russia

^b Department of Ceramics and Glass Engineering, CICECO, University of Aveiro, 3810-193 Aveiro, Portugal

ARTICLE INFO

Article history:

Received 9 February 2010

Received in revised form 1 April 2010

Accepted 4 May 2010

Available online 12 May 2010

Keywords:

X-ray diffraction

Thermogravimetric analysis

Thermal expansion

ABSTRACT

Layered $\text{LnBaCo}_2\text{O}_{5+\delta}$ (Ln = Nd, Sm) with the cation-ordered double perovskite structure were synthesized by the solid-state reaction route and characterized by X-ray diffraction, thermogravimetric analysis and dilatometry. For $\text{NdBaCo}_2\text{O}_{5.73}$ and $\text{SmBaCo}_2\text{O}_{5.61}$ equilibrated with atmospheric oxygen at low temperatures, tetragonal and orthorhombic polymorphs were found to form, respectively. The oxygen content at 300–1300 K decreases with decreasing rare-earth cation size, whilst δ variations and chemical contribution to the apparent thermal expansion in air are substantially lower compared to the disordered (Ln, A) $\text{CoO}_{3-\delta}$ (A = Ca, Sr) analogues. The average thermal expansion coefficients are $23.1 \times 10^{-6} \text{ K}^{-1}$ for $\text{NdBaCo}_2\text{O}_{5+\delta}$ and $20.8 \times 10^{-6} \text{ K}^{-1}$ for $\text{SmBaCo}_2\text{O}_{5+\delta}$ at 300–1370 K and atmospheric oxygen pressure. These values are comparable to those of Bi_2O_3 -based ionic conductors, but are incompatible with common electrolytes such as stabilized zirconia or doped ceria. The oxygen partial pressure dependencies of the total conductivity and Seebeck coefficient, studied in the $P(\text{O}_2)$ range from 10^{-10} to 1 atm, confirm predominant p-type electronic conductivity.

© 2010 Elsevier Ltd. All rights reserved.

1. Introduction

Barium- and rare-earth-containing cobaltites $\text{LnBaCo}_2\text{O}_{5+\delta}$, which belong to the family of cation-ordered double perovskites with general formula $\text{AA}'\text{B}_2\text{O}_{5+\delta}$, attract significant interest due to a variety of electrical, magnetic and physicochemical properties unusual for their disordered analogues with $\text{ABO}_{3-\delta}$ perovskite structure [1–13]. Contrary to the Sr- and Ca-substituted cobaltite systems where $\text{Ln}_{1-x}\text{A}_x\text{CoO}_{3-\delta}$ solid solutions exist at moderate radii of Ln^{3+} cations (e.g., for Ln = Pr–Gd), the introduction of barium at $x = 0.5$ leads to the formation of $\text{LnBaCo}_2\text{O}_{5+\delta}$ with the separation of Ba^{2+} and Ln^{3+} planes in the crystal lattice. The properties of $\text{LnBaCo}_2\text{O}_{5+\delta}$ are strongly dependent on the structural features and oxygen stoichiometry, varying with temperature and oxygen partial pressure, $P(\text{O}_2)$. Nonetheless, the use of similar preparation conditions yields similar structural types and oxygen content ($5 + \delta$) (Table 1). In particular, the literature data summarized in Table 1 show that under ambient conditions, neodymium cobaltite $\text{NdBaCo}_2\text{O}_{5+\delta}$ possesses a tetragonal $a_p \times a_p \times 2a_p$ structure where a_p is cubic perovskite unit cell parameter (so-called “1 1 2”-structure, space group $P4/mmm$). The samarium-containing analogue, $\text{SmBaCo}_2\text{O}_{5+\delta}$, forms an orthorhombic phase (so-called “1 2 2”-structure, S.G. $Pmmm$) under

similar conditions; doubling of the b parameter is associated with ordering of the oxygen vacancies when the $(5 + \delta)$ values are close to 5.5. Note that, for all rare-earth double perovskites, decreasing oxygen content from 6 down to 5 causes a series of structural transformation in the sequence “tetragonal–orthorhombic–tetragonal” [2,6,8]. The ranges where the orthorhombic phase (“1 2 2” structure) was reported to be stable, correspond to $5.21 \leq (5 + \delta) < 5.6$ [2] or $5.16 \leq (5 + \delta) \leq 5.76$ [7], at least for the neodymium system. However the values of oxygen content in double perovskites obtained at approximately same conditions (all samples were cooled to room temperature in air) vary significantly, i.e., from 5.47 [5] to 5.85 [6] for Ln = Nd and from 5.4 [1] to 5.69 [6] for Ln = Sm (see Table 1). An important potential application of $\text{LnBaCo}_2\text{O}_{5+\delta}$ (Ln = Pr, Sm, Nd, Gd) is related to the electrodes of solid oxide fuel cells (SOFCs) [11–13]. Although information on mixed ionic–electronic conductivity and thermomechanical properties of $\text{LnBaCo}_2\text{O}_{5+\delta}$ is still scarce, the available literature data (e.g. Refs. [7,10–13]) indicate serious advantages of these materials with respect to disordered $\text{Ln}_{1-x}\text{A}_x\text{CoO}_{3-\delta}$ perovskites. Such advantages include, in particular, a fast oxygen exchange and diffusion, a substantially high electronic conductivity and moderate thermal expansion in the intermediate-temperature range. Again, these properties are all dependent on the oxygen content and structural ordering [7,10–13].

The present work was focused on the analysis of oxygen nonstoichiometry, electrical properties and thermal expansion of $\text{LnBaCo}_2\text{O}_{5+\delta}$ (Ln = Sm, Nd) at elevated temperatures.

* Corresponding author. Tel.: +7 343 261 74 11; fax: +7 343 261 74 11.
E-mail address: Vladimir.cherepanov@usu.ru (V.A. Cherepanov).

Table 1
Summary on the crystal structure and oxygen stoichiometry of $\text{LnBaCo}_2\text{O}_{5+\delta}$ ($\text{Ln}=\text{Nd}, \text{Sm}$) prepared in various conditions.

Final annealing temperature and cooling rate	Structure	$5+\delta$	Structure	$5+\delta$	Ref.
	$\text{NdBaCo}_2\text{O}_{5+\delta}$		$\text{SmBaCo}_2\text{O}_{5+\delta}$		
1373 K, slowly cooled down to room temperature	112 by XRD ^a 122 by ED ^b	5.7	112 by XRD 122 by ED	5.4	[1]
1373 K, quenched in air during 2–3 min	Tetragonal	5.62(4)	Orthorhombic	5.54(6)	[2]
1373 K (no information on cooling rate)	$P4/mmm$ tetragonal	5.78	$Pmmm$ orthorhombic	5.65	[3]
1373 K, slowly cooled down to room temperature	–	5.75	–	–	[4]
1273–1423 K, cooled down to room temperature	$Pmmm$	5.47	–	–	[5] and references cited
1173 K, slowly cooled to room temperature at a rate of 1 °C/min	$P4/mmm$	5.85	$Pmmm$	5.69	[6]
1273 K, slowly cooled down to room temperature	tetragonal 112	5.65–5.7	orthorhombic –	–	[7]

^a X-ray diffraction.

^b Electron diffraction.

2. Experimental

The polycrystalline samples $\text{LnBaCo}_2\text{O}_{5+\delta}$ ($\text{Ln}=\text{Nd}, \text{Sm}$) were synthesized by a solid-state reaction using Nd_2O_3 , Sm_2O_3 , BaCO_3 and Co_3O_4 as starting materials. Preliminary annealed starting materials were mixed in stoichiometric ratios and grounded in an agate mortar. Two first annealing cycles were performed at 1123 K and 1223 K; then the samples were fired at 1373 K for 120 h in air with intermediate grindings and slowly cooled down to room temperature with a rate of approximately 1.5 K/min. The synthesized materials were characterized by X-ray diffraction (XRD) analysis using a Rigaku D/Max-B instrument ($\text{Cu K}\alpha$ radiation, $2\theta = 10\text{--}100^\circ$, step 0.02° , 10 s/step). Structural parameters were refined using Fullprof software. Dense ceramic samples were obtained by uniaxial pressing and sintering at 1473 K in air for 12 h, with subsequent slow cooling (~ 1.5 K/min). The density of

the polished ceramic samples was not less than 90% of their theoretical density calculated from the XRD data. The absence of open porosity and microstructural defects, such as cracks and compositional inhomogeneities, was confirmed by scanning electron microscopy coupled with energy-dispersive spectroscopy (SEM/EDS, JEOL JSM-6390LA microscope, JED-2300 analyzer). Thermal expansion was measured using a Netzsch DIL 402C dilatometer in the temperature range 300–1373 K in air, with the cooling/heating rate 5 K/min. The total electrical conductivity (σ , 4-probe DC) and Seebeck coefficient were studied in the oxygen partial pressure range 10^{-10} to 1 atm using an automatic setup equipped with an electrochemical oxygen pump and a sensor, both made of $\text{ZrO}_2(\text{Y}_2\text{O}_3)$ solid electrolyte ceramics. The Seebeck coefficient values were measured under a temperature gradient of ~ 10 K/cm, and were then corrected for thermopower of Pt leads. The total oxygen content at atmospheric oxygen pressure was determined by thermogravimetric analysis of powdered samples (TGA, Setaram SetSys 16/18, weight resolution of 0.4 μg ; sample weight of 650–800 mg). The TGA procedures included both heating and cooling with a constant rate (2 K/min) in flowing dry air, and temperature cycling in the range 973–1323 K with 50 K steps and equilibration at each temperature during 3 h as illustrated in Fig. 1A. After the measurements in air, the apparatus was flushed with argon at 1323 K and the samples were reduced in a flow of dried 10% H_2 –90% N_2 mixture for 10 h, with subsequent heating up to 1423 K in the same flow in order to ensure complete reduction of cobalt (Fig. 1B). The experimental procedures, equipment and equilibration criteria were reported in previous works (e.g., Refs. [14–16] and references cited).

3. Results and discussion

XRD analysis of $\text{LnBaCo}_2\text{O}_{5+\delta}$ ($\text{Ln}=\text{Nd}, \text{Sm}$) showed formation of single phases with the double perovskite structure. The equilibration with atmospheric oxygen was confirmed by TGA. In particular, the oxygen content variations observed in the regimes of continuous cooling and isothermal dwells display an excellent agreement (Fig. 2), suggesting that the oxygen exchange processes and, hence, equilibration are fast enough. The same conclusion can be drawn considering the transient behavior illustrated in Fig. 1. This coincides well with literature data on $\text{GdBaCo}_2\text{O}_{5+\delta}$ [11,12]. On cooling, $\text{LnBaCo}_2\text{O}_{5+\delta}$ ($\text{Ln}=\text{Nd}, \text{Sm}$) exhibit a typical mass saturation, which occurs at approximately 530 K in both cases. No oxygen absorption characteristic of non-equilibrium oxygen content was observed during further heating.

Another important conclusion is that the oxygen content decreases with decreasing size of the lanthanide cations. At room temperature, the values of δ in $\text{LnBaCo}_2\text{O}_{5+\delta}$ decrease from ~ 0.73 for $\text{Ln}=\text{Nd}$ down to ~ 0.61 for Sm . These TGA results are in a good agreement with data reported in Refs. [1,3] for $\text{NdBaCo}_2\text{O}_{5+\delta}$ and

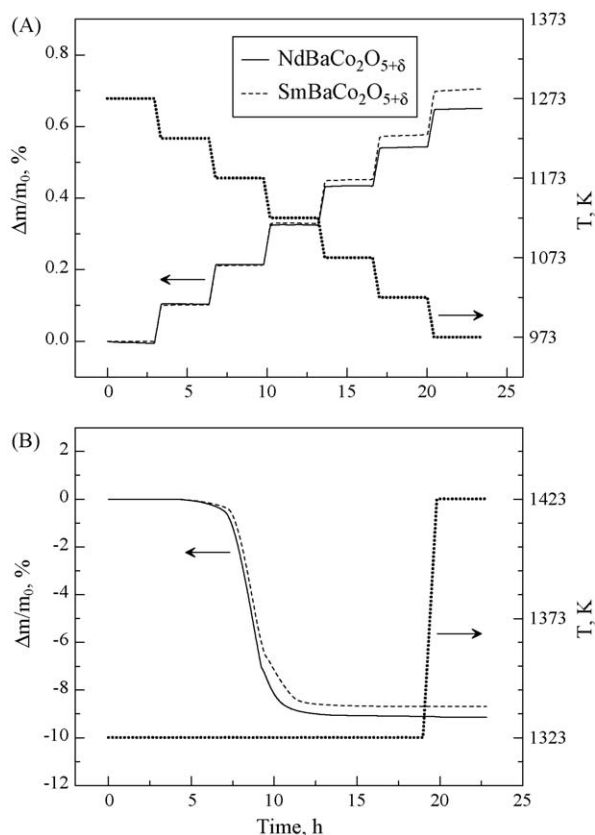


Fig. 1. Relative weight variations of powdered $\text{LnBaCo}_2\text{O}_{5+\delta}$ samples on temperature cycling in air (A), and on reduction (B).

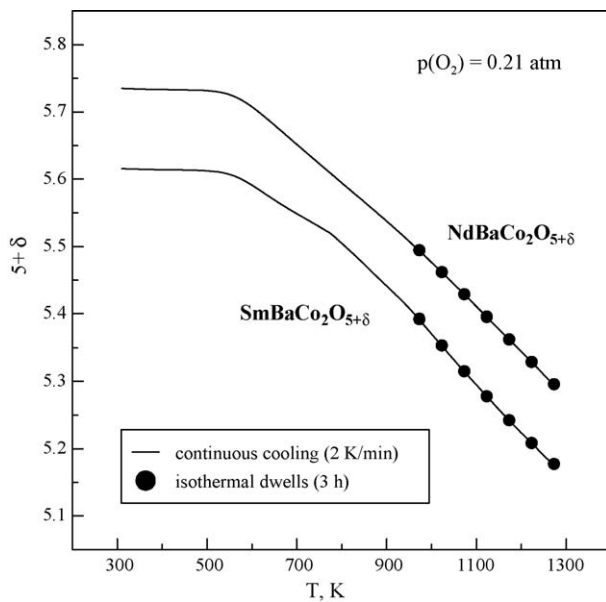


Fig. 2. Variations of oxygen content in $\text{LnBaCo}_2\text{O}_{5+\delta}$ in air.

[2,3] for $\text{SmBaCo}_2\text{O}_{5+\delta}$. Notice that a very similar trend was recently revealed for cation-disordered $(\text{Ln}, \text{Sr})\text{FeO}_{3-\delta}$ perovskites [16]. The values of oxygen content, obtained in Ref. [5] for $\text{Ln} = \text{Nd}$ and [1] for $\text{Ln} = \text{Sm}$, were either too understated or the samples used were not fully equilibrated during the cooling process, and reported in Ref. [6] for $\text{Ln} = \text{Nd}$ seems to be overestimated.

According to the results of Rietveld refinement, XRD patterns of $\text{NdBaCo}_2\text{O}_{5+\delta}$ can be indexed on the basis of an $a_p \times a_p \times 2a_p$ tetragonal unit cell (S.G. $P4/mmm$). The experimental and calculated profiles are shown in Fig. 3A. For $\text{SmBaCo}_2\text{O}_{5+\delta}$, XRD reveals splitting of the peaks at 22.72° and 46.47° (Fig. 3B), thus indicating changing the lattice symmetry from tetragonal to orthorhombic ($a_p \times 2a_p \times 2a_p$, S.G. $Pmmm$). These results agree well with the literature data [1–9] summarized in Table 1. One should mention that doubling of the b parameter in the case of $\text{SmBaCo}_2\text{O}_{5+\delta}$ is caused by ordering of the oxygen vacancies located in the Sm-containing layers [1] and correlates with the higher vacancy concentration (Fig. 2). The unit cell parameters and the refined atomic parameters are presented in Tables 2 and 3, respectively.

The thermal expansion behavior of $\text{LnBaCo}_2\text{O}_{5+\delta}$ ($\text{Ln} = \text{Nd}, \text{Sm}$) ceramics is illustrated in Fig. 4; Table 4 lists the thermal expansion coefficients (TECs) calculated from the dilatometric data and averaged in the temperature range 300–1373 K. At temperatures below 1000 K, both materials exhibit very similar expansion; on further heating, the larger oxygen losses from $\text{NdBaCo}_2\text{O}_{5+\delta}$ lattice (Fig. 2) lead to higher chemical contribution to the volume variations. As a result, the average TEC of $\text{NdBaCo}_2\text{O}_{5+\delta}$, $23 \times 10^{-6} \text{ K}^{-1}$, becomes higher than that of $\text{SmBaCo}_2\text{O}_{5+\delta}$, $21 \times 10^{-6} \text{ K}^{-1}$. Both values are slightly larger than those presented in earlier publication [3], but in our work measurements were

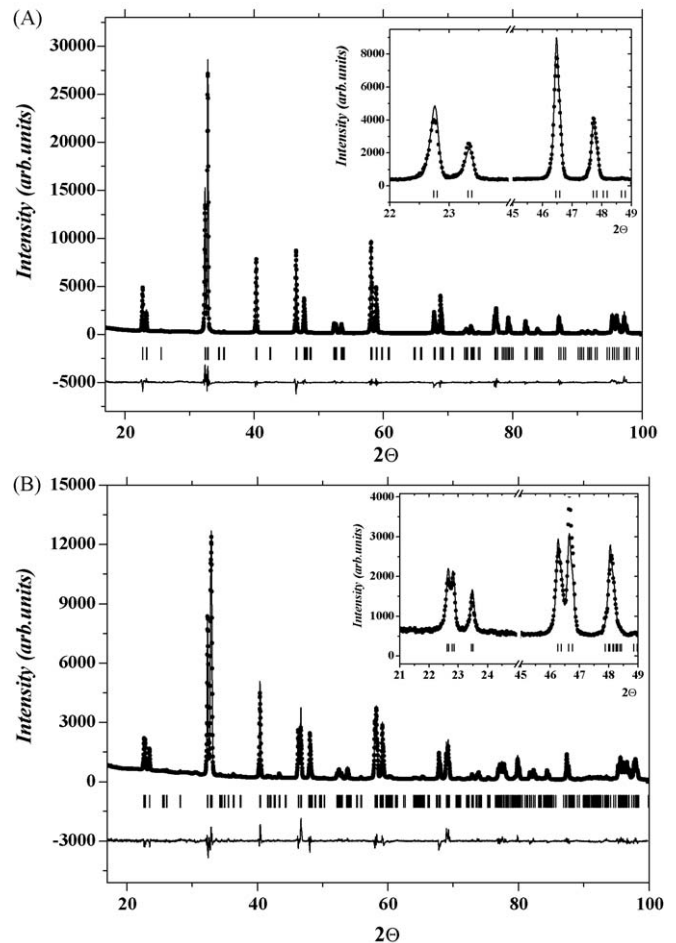


Fig. 3. Rietveld refinement profiles of $\text{NdBaCo}_2\text{O}_{5+\delta}$ (A) and $\text{SmBaCo}_2\text{O}_{5+\delta}$ (B). The circles and upper continuous plot correspond to the experimental data points and calculated profile, respectively. The lower line is the difference plot. The inserts show an absence (A) and appearance (B) of splitting of the peak at $\sim 22\text{--}23^\circ$.

made in a wider temperature range (300–1373 K). It is easy to see (Fig. 2) that the slope of dilatometric curves increases with the increase of temperature. Even in publication [3] the values of TEC obtained for the temperature range 500–900 °C are larger than those calculated within 80–900 °C. Nevertheless, these values and the oxygen vacancy concentration variations in $\text{LnBaCo}_2\text{O}_{5+\delta}$ are substantially lower compared to the cobaltites with cation-disordered perovskite lattice, where the chemical expansion on heating is much higher and the TECs achieve $(25\text{--}35) \times 10^{-6} \text{ K}^{-1}$ (e.g., see Refs. [17,18] and references therein).

Fig. 5 presents the isothermal dependences of electrical conductivity versus oxygen partial pressure ($\log \sigma - \log P(\text{O}_2)$) and Seebeck coefficient ($Q - \log P(\text{O}_2)$) for $\text{NdBaCo}_2\text{O}_{5+\delta}$. Decreasing oxygen pressure results in a lower conductivity, whilst the thermopower increases and remains positive in the whole $P(\text{O}_2)$

Table 2
Unit cell parameters and agreement factors.

Parameters	a (Å)	b (Å)	c (Å)	V (Å) ³	Oxygen content	Refinement parameters
$\text{NdBaCo}_2\text{O}_{5+\delta}$	3.903(1)	3.903(1)	7.614(1)	116.02(2)	5.73	$R_{\text{Br}} = 5.88\%$ $R_{\text{p}} = 8.54\%$ $R_{\text{exp}} = 4.23\%$
$\text{SmBaCo}_2\text{O}_{5+\delta}$	3.886(1)	7.833(1)	7.560(1)	230.22(2)	5.61	$R_{\text{Br}} = 10.7\%$ $R_{\text{p}} = 7.73\%$ $R_{\text{exp}} = 4.46\%$

Table 3
Structural parameters for LnBaCo₂O_{5+δ} obtained from Rietveld refinement.

S.G. P4/mmm				S.G. Pmmm			
Atom	x	y	z	Atom	x	y	z
Nd (1d)	0.5	0.5	0.5	Sm (2p)	0.5	0.229(3)	0.5
Ba (1c)	0.5	0.5	0	Ba (2o)	0.5	0.250(1)	0
Co1 (2g)	0	0	0.252(1)	Co1 (2q)	0	0.5	0.255(2)
O1 (1a)	0	0	0	Co2 (2r)	0	0	0.254(2)
O2 (1b)	0	0	0.5	O1 (1a)	0	0	0
O3 (4i)	0	Occ. = 0.674(3)	0.281(2)	O2 (1e)	0	0.5	0
				O3 (1g)	0	0.5	0.5
				O4 (1c)	0	0	0.5
						Occ. = 0.249(5)	
						Occ. = 0.929(6)	
				O5 (2s)	0.5	0	0.239(3)
				O6 (2t)	0.5	0.5	0.247(3)
				O7 (4u)	0	0.244(2)	0.238(2)

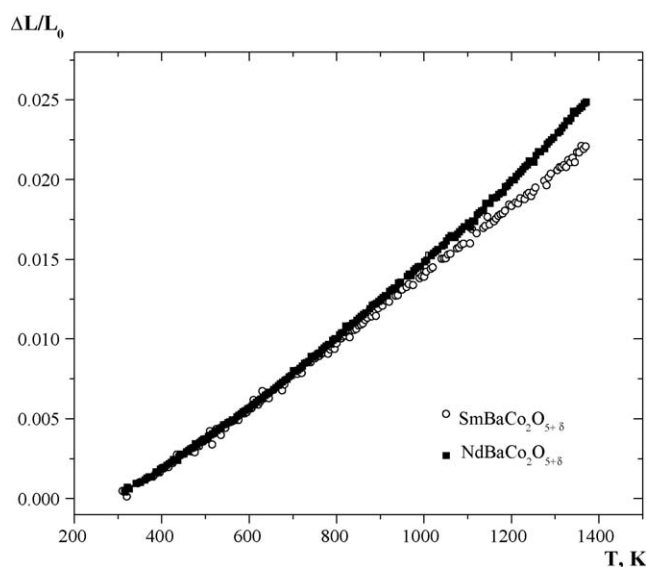


Fig. 4. Linear thermal expansion of LnBaCo₂O_{5+δ} ceramics in air.

range studied. These trends unambiguously indicate that the electronic transport is p-type, as for PrBaCo₂O_{5+δ} [10], SmBaCo₂O_{5+δ} [13] and GdBaCo₂O_{5+δ} [19]. The conductivity values vary in the range 150–400 S/cm, which is very close to other cobaltites with the double perovskite structure and is sufficient for applications in the SOFC cathodes.

In summary, whilst the oxygen vacancy concentration in LnBaCo₂O_{5+δ} (Ln = Nd, Sm) is higher with respect to cation-disordered (Ln, A)CoO_{3-δ} (A = Ca, Sr) [17,18], the oxygen content variations in the double perovskites at temperatures up to 1370 K in air are considerably lower. This leads to significantly lower average TECs which comprise significant chemical contributions due to cobalt radius changes. Consequently, LnBaCo₂O_{5+δ} display almost linear dilatometric curves. As for the oxygen stoichiometry variations, the chemical expansion decreases with decreasing Ln³⁺ cation size. At the same time, the average TECs of LnBaCo₂O_{5+δ} are still high $(20.8\text{--}23.1) \times 10^{-6} \text{ K}^{-1}$ at 300–1370 K. These values are only compatible with Bi₂O₃-based solid electrolytes, such as Bi₂V_{0.9}Cu_{0.1}O_{5.5-δ}, and incompatible with common solid electro-

Table 4
Average thermal expansion coefficients (TECs) of LnBaCo₂O_{5+δ} in air.

Composition	T (K)	TEC ($\times 10^6 \text{ K}^{-1}$)
NdBaCo ₂ O _{5+δ}	298–1373	23.1 ± 0.1
SmBaCo ₂ O _{5+δ}	298–1373	20.80 ± 0.06

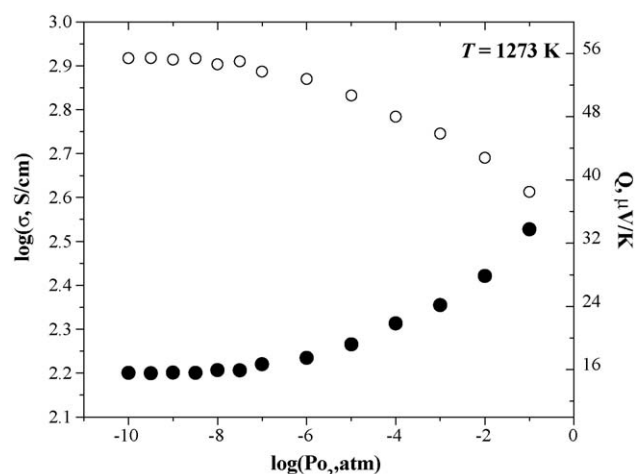


Fig. 5. Oxygen partial pressure dependences of the electrical conductivity (filled symbols) and Seebeck coefficient (open symbols) of NdBaCo₂O_{5+δ} at 1273 K.

lytes such as yttria-stabilized zirconia or gadolinia-doped ceria [18].

Acknowledgments

This work was financially supported in parts by RFBR grant no. 09-03-00620, Federal Agency for Science and Innovations of Russian Federation, Federal Agency for Education of Russian Federation, and the FCT, Portugal (project PTDC/CTM/64357/2006).

References

- [1] A. Maignan, C. Martin, D. Pelloquin, N. Nguyen, B. Raveau, J. Solid State Chem. 142 (1999) 247–260.
- [2] P.S. Anderson, C.A. Kirk, J. Knudsen, I.M. Reaney, A.R. West, Solid State Sci. 7 (2005) 1149–1156.
- [3] J.-H. Kim, A. Manthiram, J. Electrochem. Soc. 155 (4) (2008) B385–B390.
- [4] M. Karppinen, M. Matvejeff, K. Salomäki, H. Yamauchi, J. Mater. Chem. 12 (2002) 1761–1764.
- [5] F. Fauth, E. Suard, V. Caignaert, I. Mirebeau, Phys. Rev. B 66 (2002) 184421.
- [6] J.-H. Kim, L. Moggi, F. Prado, A. Caneiro, J.A. Alonso, A. Manthiram, J. Electrochem. Soc. 156 (12) (2009) B1376–B1382.
- [7] V. Pralong, V. Caignaert, S. Hebert, A. Maignan, B. Raveau, Solid State Ionics 177 (2006) 1879–1881.
- [8] J.F. Mitchell, J. Burley, S. Short, J. Appl. Phys. 93 (10) (2003) 7364–7366.
- [9] J.C. Burley, J.F. Mitchell, S. Short, D. Miller, Y. Tang, J. Solid State Chem. 170 (2003) 339–350.
- [10] S. Streule, A. Podlesnyak, D. Sheptyakov, E. Pomjakushina, M. Stingaciu, K. Conder, M. Medarde, M.V. Patrakeev, I.A. Leonidov, V.L. Kozhevnikov, J. Mesot, Phys. Rev. B 73 (2006) 094203.
- [11] A.A. Taskin, A.N. Lavrov, Y. Ando, Appl. Phys. Lett. 86 (2005) 091910.

- [12] A. Tarascon, S.J. Skinner, R.J. Chater, F. Hernandez-Ramirez, J.A. Kilner, J. Mater. Chem. 17 (2007) 3175–3181.
- [13] J.H. Kim, Y. Kim, P.A. Connor, J.T.S. Irvine, J. Bae, W. Zhou, J. Power Sources 194 (2009) 704–711.
- [14] I.A. Leonidov, V.L. Kozhevnikov, E.B. Mitberg, M.V. Patraeev, V.V. Kharton, F.M.B. Marques, J. Mater. Chem. 11 (2001) 1202–1209.
- [15] E.V. Tsipis, M.V. Patraeev, J.C. Waerenborgh, Y.V. Pivak, A.A. Markov, P. Gaczyński, E.N. Naumovich, V.V. Kharton, J. Solid State Chem. 180 (2007) 1902–1910.
- [16] V.V. Kharton, A.V. Kovalevsky, M.V. Patraeev, E.V. Tsipis, A.P. Viskup, V.A. Kolotygin, A.A. Yaremchenko, A.L. Shaula, E.A. Kiselev, J.C. Waerenborgh, Chem. Mater. 20 (2008) 6457–6467.
- [17] A.N. Petrov, V.A. Cherepanov, A.Yu. Zuev, J. Solid State Electrochem. 10 (2006) 517–537.
- [18] E.V. Tsipis, V.V. Kharton, J. Solid State Electrochem. 12 (2008) 1367–1391.
- [19] M.-B. Choi, S.-Y. Jeon, J.-S. Lee, H.-J. Hwang, S.-J. Song, J. Power Sources 195 (2010) 1059–1064.